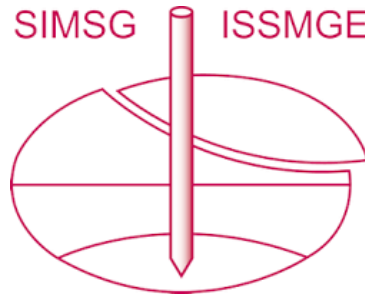


INTERNATIONAL SOCIETY FOR SOIL MECHANICS AND GEOTECHNICAL ENGINEERING



This paper was downloaded from the Online Library of the International Society for Soil Mechanics and Geotechnical Engineering (ISSMGE). The library is available here:

<https://www.issmge.org/publications/online-library>

This is an open-access database that archives thousands of papers published under the Auspices of the ISSMGE and maintained by the Innovation and Development Committee of ISSMGE.

The paper was published in the proceedings of the 10th European Conference on Numerical Methods in Geotechnical Engineering and was edited by Lidija Zdravkovic, Stavroula Kontoe, Aikaterini Tsiampousi and David Taborda. The conference was held from June 26th to June 28th 2023 at the Imperial College London, United Kingdom.

To see the complete list of papers in the proceedings visit the link below:

<https://issmge.org/files/NUMGE2023-Preface.pdf>

Extended subloading surface anisotropic model for cyclic behaviour of structured clays

H. Dejaloud, M. Rezania

School of Engineering, University of Warwick, Coventry, UK

ABSTRACT: In this paper, an advanced kinematic hardening multi-surface constitutive model is proposed for studying the cyclic response of structured clayey soils by extending the well-known S-CALY1S model using the concept of the extended subloading surface. In addition to the isotropic, rotational and destructuration hardening rules, the developed model is enhanced with a kinematic hardening law that controls the movement of the subloading inside the normal yield surface due to the resultant plastic strain increments. The adopted extended subloading surface formulation enables the model to reproduce a more realistic representation of the nonlinear behaviour of clays, with different overconsolidation ratios, under the application of both monotonic and cyclic loadings. The model formulation is presented and some of the capabilities of the proposed model are demonstrated through a number of numerical examples. The developed model shows satisfactory predictions of some important aspects of observed response during cyclic loading of natural clays such as shear modulus reduction and damping ratio, degradation index, and stress-strain responses.

Keywords: Constitutive modelling, Clay, Cyclic behaviour, subloading surface plasticity

1 INTRODUCTION

Characterizing the behaviour of clays under the application of cyclic loadings (e.g., earthquake, wave-induced, traffic-induced, machine vibration, etc.) is of critical importance in many geotechnical applications. Regarding this, developing a constitutive model that is capable to capture the cyclic behaviour of clays has been a topic of extensive research over the past few decades, and different theories have been proposed. Besides the bounding surface concept that was developed first by Dafalias and Popov (1975) (Rezania et al., 2014; Rezania and Dejaloud, 2021), the extended subloading surface method (Hashiguchi 1989) has gained a considerable reputation for enhancing the conventional elastoplastic constitutive models to replicate cyclic behaviour.

Taking advantage of using multiple surfaces, the extended subloading surface concept leads to smoothed emergence of plastic behaviour during the shearing and provides the capability to simulate cyclic loadings. In this concept, the stress state inside the yield surface (which is called normal-yield surface in this theorem) is carried by a floating subloading surface. In addition to the hardening rules associated with the host conventional elastoplastic model (e.g., isotropic and rotational hardening), the extended subloading surface adds two more hardening rules that control the size and position of the subloading surface inside the normal-yield surface.

In this paper, the well-known S-CLAY1S (Karstunen et al., 2005) model is enhanced with the extended

subloading surface concept to provide a more realistic representation of clay behaviour under the application of cyclic loads. In the following sections, each of the model components is introduced in the triaxial stress space.

It must be noted that all stress-related parameters used in this paper represent effective stresses, and the prime sign is therefore neglected.

2 MODEL FORMULATION

2.1 Normal-yield surface

The normal-yield surface represents the maximum combination of the principal stresses that soil has experienced throughout its history. In the proposed model, this surface is an oriented ellipsoid and is expressed by

$$f = (q - \alpha p)^2 - (M^2 - \alpha^2)(p_0 - p)p = 0 \quad (1)$$

where α is a stress-ratio type variable that defines the inclination of the yield surface to represent the plastic anisotropy, p_0 is pre-consolidation pressure and represents the size of the yield surface, M is the slope of the critical state line (CSL), and p and q are mean effective and deviatoric stresses, respectively.

In order to account for the effect of bonding, according to Gens and Nova (1993), the size of the normal-yield surface can be related to the one of the intrinsic normal-yield surface (p_{0i}) as follows

$$p_0 = (1 + x)p_{0i} \quad (2)$$

where x governs the amount of bonding/structure.

2.2 Subloading surface and elastic-core surfaces

The subloading surface can be considered as the projection of the normal-yield surface from the similarity centre (p_c and q_c) which is located on the elastic-core surface and with the scale of R which is called the normal-yield ratio. The elastic-core surface passes from the origin of the stress space and is defined as follows

$$f_c = (q_c - \alpha p_c)^2 - (M^2 - \alpha^2)(R_c p_0 - p_c)p_c = 0 \quad (3)$$

in which the superscript c is to emphasise the stress quantities associated with the similarity centre, and R_c is the ratio of the size of the elastic-core surface to that of the normal-yield surface.

The position of the subloading surface's reference point can be anchored to the similarity centre via

$$\begin{aligned} p_b &= (1 - R)p_c \\ q_b &= (1 - R)q_c \end{aligned} \quad (4)$$

Considering a local stress space coordinate system attached to the origin of the subloading surface, point B in Figure 1, the subloading surface can be mathematically expressed as

$$\bar{f} = (\bar{q} - \alpha \bar{p})^2 - (M^2 - \alpha^2)(R p_0 - \bar{p})\bar{p} = 0 \quad (5)$$

the bar sign ($\bar{\quad}$) represents the stress quantities in the local stress space coordinate system (i.e., $\bar{\sigma} = \sigma - \sigma_c$).

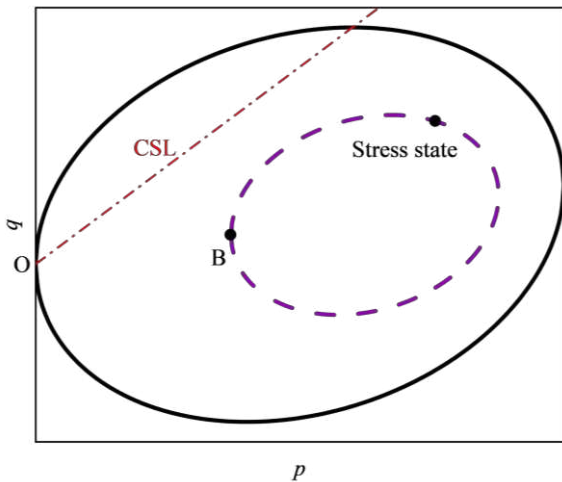


Figure 1. Normal-yield (solid ellipsoid) and floating subloading (dashed ellipsoid) of the proposed model

Moreover, since the associated flow rule is adopted in the proposed model, the plastic potential surface is

considered to be identical to the floating subloading surface, i.e., $g = \bar{f}$.

2.3 Hardening rules

2.3.1 Isotropic hardening rule

Similar to the S-CLAY1 model, any change in the size of the normal-yield surface is directly related to the plastic volumetric strain ($d\varepsilon_v^p$), as

$$dp_0 = \frac{vp_0}{\lambda - \kappa} d\varepsilon_v^p \quad (6)$$

in which v is the specific volume, λ and κ are the slopes of the normal compression and swelling lines in the ($\ln p - v$) space, respectively.

2.3.2 Rotational hardening rule

The proposed model uses the same rotational hardening rule as adopted in the S-CLAY1S model to simulate the rotation of the normal-yield surface during strainings. The rotational hardening formulation represents the development and elimination of anisotropy due to both plastic volumetric and deviatoric strain increments ($d\varepsilon_d^p$), and is expressed by the following equation in the triaxial stress space

$$d\alpha = \mu \left[\frac{3\eta}{4} - \alpha \right] \langle d\varepsilon_v^p \rangle + \beta \left[\frac{\eta}{3} - \alpha \right] |d\varepsilon_d^p| \quad (7)$$

in which $\eta = q/p$ is called stress ratio, and μ and β are model parameters where the first one controls the absolute rate at which the yield surface rotates toward its equilibrium state value and the latter controls the relative effect of $d\varepsilon_d^p$ and $d\varepsilon_v^p$ in evolving the yield surface. Moreover, $\langle \rangle$ refers to Macaulay brackets. As explained by Wheeler et al. (2003), this parameter can be determined in the same way as in S-CLAY1S

$$\beta = \frac{3(4M^2 - 4\eta_{K_0}^2 - 3\eta_{K_0})}{4(\eta_{K_0}^2 - M^2 + 2\eta_{K_0})} \quad (8)$$

where η_{K_0} is the stress ratio associated with the K_0 condition.

2.3.3 Destructuration

This hardening rule governs the effect of bonding degradation due to shearings. Both plastic volumetric and deviatoric strains tend to reduce the bonding parameter (x) to zero by

$$dx = -ax(|d\varepsilon_v^p| + b|d\varepsilon_d^p|) \quad (9)$$

where a and b control the absolute rate of destructuration and relative effectiveness of plastic strain components in degrading the internal bondings, respectively.

The procedure to determine these parameters is discussed in Karstunen et al. (2005).

2.3.4 Evolution of normal-yield ratio

In the proposed model, any variation of the normal-yield ratio is determined using the absolute value of the plastic strain increment which can be read as

$$dR = U(R)|d\varepsilon^p| \quad (10)$$

and

$$U(R) = u_0 \cot\left(\frac{\pi}{2} R^n\right) \quad (11)$$

where u_0 and n are model parameters. This equation helps the normal-yield ratio evolve in an appropriate way to satisfy all the conditions associated with the subloading surface theory which can be schematically seen in Figure 2.

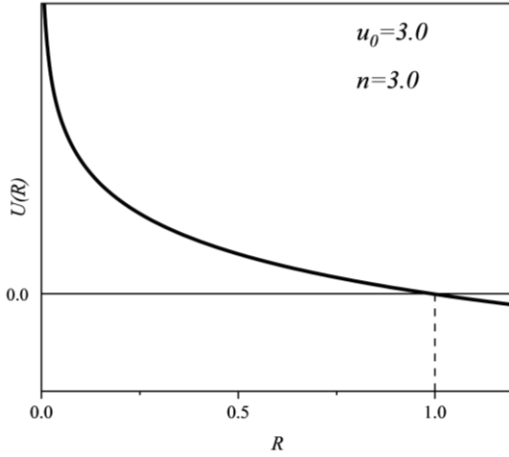


Figure 2. Variation of $U(R)$ with normal-yield ratio

2.3.5 Kinematic hardening rule

As mentioned in Equation (3), the reference point of the subloading surface is anchored to the similarity centre in the stress space. Therefore, the movement of the subloading surface is related to both the variation of the similarity centre and normal-yield ratio. Regarding this, kinematic hardening can be formulated as

$$d\sigma_b = (1 - R)d\sigma_c - dR \sigma_c \quad (12)$$

In line with the assumptions made by Hashiguchi et al. (2022), the variation of the similarity centre is determined with the aid of applying the consistency condition on the elastic-core surface and can be expressed by the following equation

$$d\sigma_c = c_e \|d\varepsilon^p\| \left(\frac{R_c}{R} \bar{\sigma} - \sigma_c \right) - \left(\frac{1}{R_c p_0} \frac{\partial f_c}{\partial \alpha} d\alpha - \frac{1}{p_0} \frac{1+e_0}{\lambda-\kappa} d\varepsilon_v^p \right) \sigma_c \quad (13)$$

where c_e controls how fast the similarity centre can transmit inside the normal-yield surface. By substituting Equations (10) and (13) into Equation (12), the kinematic hardening rule can be derived.

3 MODEL VALIDATION

In this section, using available multistage undrained cyclic hollow cylinder test data on a compacted clay (Soralump and Prasomsri, 2016), the performance of the proposed model is investigated. Due to the fact that this type of test cannot be simulated using the model with triaxial formulation, the proposed model has been extended to the general stress state and has been implemented into the PLAXIS software to complete the simulation of this test. It should be noted that the presentation of the model formulation in general stress space and elaboration on the used integration scheme is beyond the scope of this paper. The values of required soil parameters are taken from Dejaloud and Rezania (2022) and are summarised in Table 1.

Table 1. Model parameters and initial state variables

Parameter	Values
λ	0.11
κ	0.023
ν	0.25
M	1.4
μ	550
β	0.7
a	8
b	0.25
u_0	20
n	3.5
c_e	200
e_0	0.54
α_0	0.0
x_0	4
p_0	400 kPa
$\{p_c, q_c\}$	$\{30, 0\}$ kPa

Figure 3 compares the experimental data with model responses for the overconsolidated sample (OCR=4) subjected to multi-stage cyclic loading. As can be seen, the adopted extended subloading surface method provides the proposed model with the capability to reproduce the cyclic behaviour with suitable accuracy. However, as discussed by Dejaloud and Rezania (2021), using normal-yield and plastic potential surfaces with flexible shapes can improve the simulations.

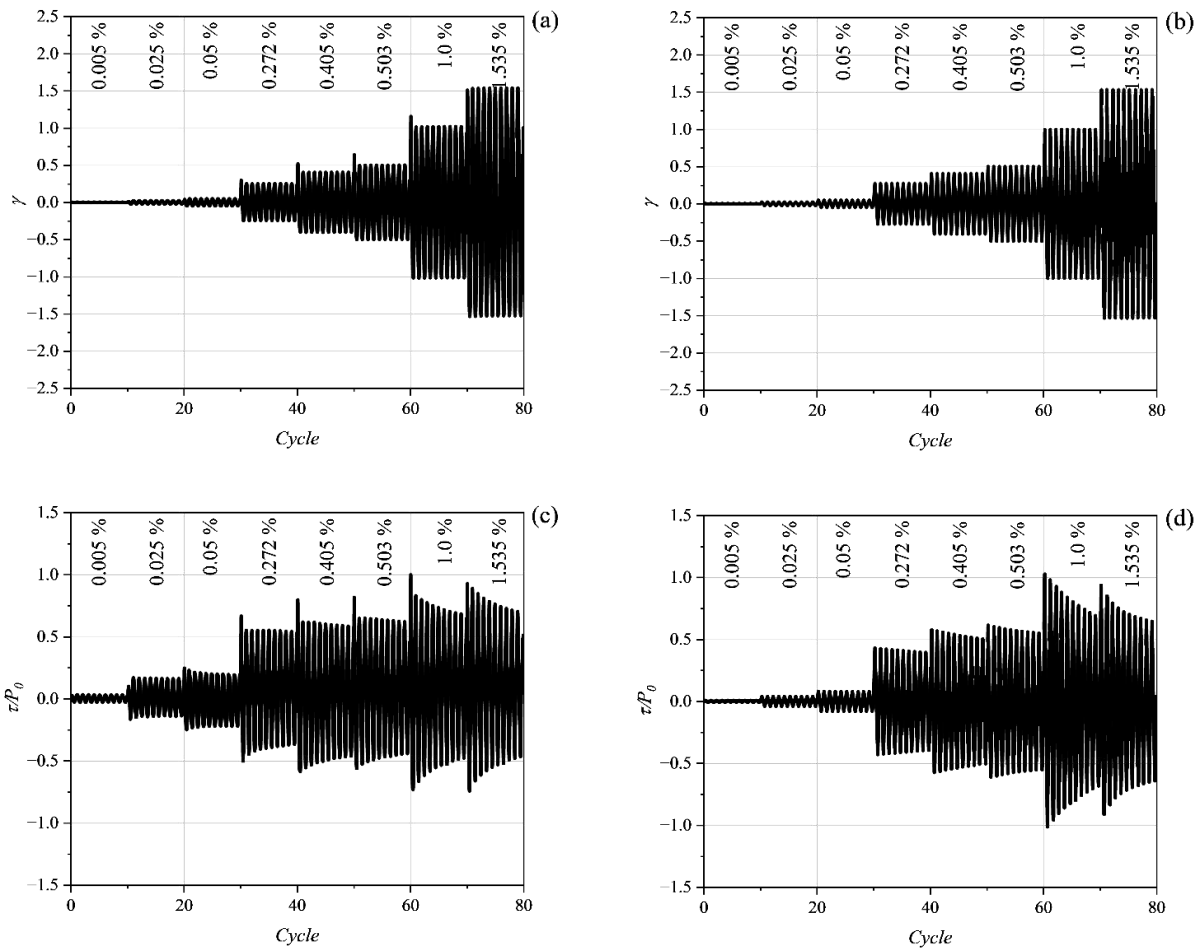


Figure 3. Comparison of multi-stage cyclic loading on overconsolidated (OCR=4) compacted clay; (a) and (c) experimental data, (b) and (d) model simulations.

Moreover, Figure 4 shows the simulated degradation index for each strain level, which is defined as follows

$$\delta = G(N)/G(1) \quad (14)$$

where $G(N)$ is secant shear modulus at cycle N , and $G(1)$ is secant shear modulus at the first cycle of each loading stage.

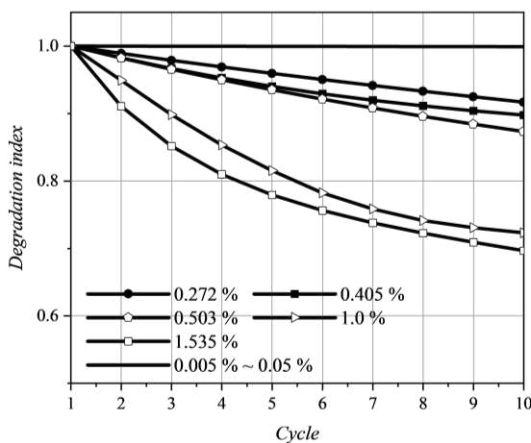


Figure 4. Simulated degradation index

In addition, the simulated shear modulus reduction (i.e., G/G_{max}) and damping ratio (D) curves for this sample are compared with the admissible ranges proposed by Vusetic and Dubry (1991) in Figure 5. The good qualitative agreement between the model simulations and proposed ranges demonstrates the adequacy of the developed extended subloading surface model to be used in the dynamic analysis of clays.

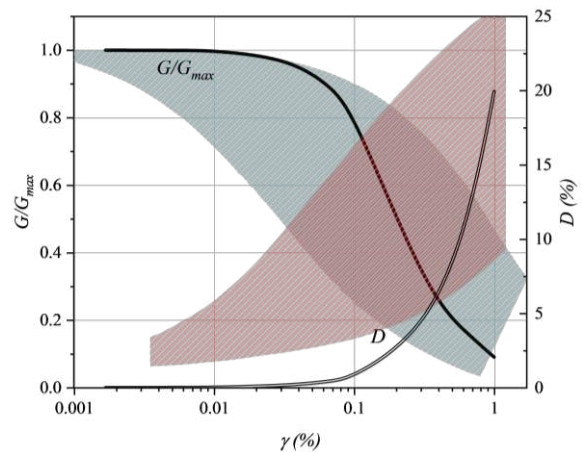


Figure 5. Shear modulus reduction and damping curves

4 CONCLUSIONS

In this paper, the well-known S-CLAY1S model was enhanced with extended subloading surface theory. By taking advantage of using multiple surfaces, the adopted concept has made the proposed model, namely ESLS-CLAY1S, capable to simulate the cyclic behaviour of structured clays. In addition to the hardening rules associated with the original version of the S-CLAY1S model, the proposed model also uses a kinematic hardening to reproduce the nonlinear behaviour when the stress state varies inside the yield surface domain. The performance of the ESLS-CLAY1S was elaborated using the data from a multi-stage cyclic hollow cylinder test on an overconsolidated compacted clay. As was shown, the proposed model demonstrates promising predictions in the stress space and also in resultant shear modulus reduction and damping ratio simulations.

5 REFERENCES

- Dafalias, Y. F., Popov, E. P. 1975. A model of nonlinearly hardening materials for complex loading. *Acta Mechanica*, **21**(3), 173–192.
- Dejaloud, H. and Rezaia, M., 2022. Double image stress point bounding surface model for monotonic and cyclic loading on anisotropic clays. *Acta Geotechnica*, pp.1-30.
- Dejaloud, H., Rezaia, M. 2021. Adaptive anisotropic constitutive modeling of natural clays. *Int. J. Numer. Analyt. Methods Geomech.* **45**, 1756–1790.
- Gens, A., Nova, R. 1993. Conceptual bases for a constitutive model for bonded soils and weak rocks. *Proc., International Symp. on Hard Soils–Soft Rocks*, Athens, Greece, 485–494
- Hashiguchi, K. 1989. Subloading surface model in unconventional plasticity. *Int. J. Solids Struct.* **25**, No. 8, 917–945.
- Hashiguchi, K., Mase, T. and Yamakawa, Y., 2022. Elaborated subloading surface model for accurate description of cyclic mobility in granular materials. *Acta Geotechnica*, **17**(3), pp.699-719.
- Karstunen, M., Krenn, H., Wheeler, S.J., Koskinen, M. and Zentar, R., 2005. Effect of anisotropy and destructuration on the behavior of Murro test embankment. *International Journal of Geomechanics*, **5**(2), pp.87-97.
- Rezaia, M., Dejaloud, H. 2021. BS-CLAY1: Anisotropic bounding surface constitutive model for natural clays. *Comput. Geotech.* **135**, p.104099.
- Rezaia, M., Dejaloud, H., Nezhad, M. M. 2014. SCLAY1S-BS: An anisotropic model for simulation of cyclic behaviour of clays. In *Geomechanics from Micro to Macro* (Eds: Soga, K., Kumar, K., Biscontin, G., Kuo, M.), 651–655. CRC Press.
- Soralump, S., Prasomsri, J. 2016. Cyclic pore water pressure generation and stiffness degradation in compacted clays. *J. Geotech. Geoenviron. Engng.* **142**, No. 1, p.04015060.
- Vucetic, M. and Dobry, R., 1991. Effect of soil plasticity on cyclic response. *Journal of geotechnical engineering*, **117**(1), pp.89-107.
- Wheeler, S.J., Näätänen, A., Karstunen, M. and Lojander, M., 2003. An anisotropic elastoplastic model for soft clays. *Canadian Geotechnical Journal*, **40**(2), pp.403-418.